Preclinical Characterization of ARX517, a Site-Specific Stable PSMA-Targeted Antibody–Drug Conjugate for the Treatment of Metastatic Castration-Resistant Prostate Cancer

Lillian K. Skidmore, David Mills, Ji Young Kim, Nick A. Knudsen, Jay D. Nelson, Manoj Pal, Jianing Wang, Kedar GC, Michael J. Gray, Wisam Barkho, Prathap Nagaraja Shastri, Mysore P. Ramprasad, Feng Tian, Daniel O'Connor, Ying J. Buechler, and Shawn Shao-Hui Zhang

ABSTRACT

Metastatic castration-resistant prostate cancer (mCRPC) is an advanced disease in which patients ultimately fail standard-of-care androgen deprivation therapies and exhibit poor survival rates. The prostate-specific membrane antigen (PSMA) has been validated as an mCRPC tumor antigen with overexpression in tumors and low expression in healthy tissues. Using our proprietary technology for incorporating synthetic amino acids into proteins at selected sites, we have developed ARX517, an antibody–drug conjugate composed of a humanized anti-PSMA antibody site-specifically conjugated to a tubulin inhibitor at a drug-to-antibody ratio of 2. After binding PSMA, ARX517 is internalized and catabolized, leading to cytotoxic payload delivery and apoptosis. To minimize premature payload release and maximize delivery to tumor cells, ARX517 employs a noncleavable polyethylene glycol linker and stable oxime conjugation enabled via synthetic amino acid protein incorporation to ensure its overall stability. *In vitro* studies demonstrate that ARX517 selectively induces cytotoxicity of PSMA-expressing tumor cell lines. ARX517 exhibited a long terminal half-life and high serum exposure in mice and dose-dependent antitumor activity in both enzalutamide-sensitive and -resistant cell line–derived xenograft and patient-derived xenograft models of prostate cancer. Repeat-dose toxicokinetic studies in nonhuman primates demonstrated that ARX517 was tolerated at exposures well above therapeutic exposures in mouse pharmacology studies, indicating a wide therapeutic index. In summary, ARX517 inhibited tumor growth in diverse mCRPC models, demonstrated a tolerable safety profile in monkeys, and had a wide therapeutic index based on preclinical exposure data. Based on the encouraging preclinical data, ARX517 is currently being evaluated in a phase I clinical trial (NCT04662580).

Introduction

Prostate cancer is the second leading cause of cancer death in men in the United States (1). Treatment options include surgery, radiotherapy, and androgen deprivation therapy. However, patients with advanced, high-risk disease eventually progress to metastatic castration-resistant prostate cancer (mCRPC) which has a median overall survival of approximately 2 years in real-world settings (2). Although approved treatments for patients with mCRPC include diverse drug classes such as taxanes, androgen receptor pathway inhibitors, targeted radioligand therapy, and PARP inhibitors (for patients with BRCA or homologous recombination repair mutations; ref. 3), patients eventually develop resistance to these treatments, and thus, novel and effective treatments are needed.

Prostate-specific membrane antigen (PSMA) is a promising prostate cancer therapeutic target with limited expression in healthy cells and high incidence of overexpression on the surface of primary prostate tumors, as well as in metastatic lesions in lymph nodes and bone (4, 5). Based on results from the VISION trial, PLUVICTO (lutetium Lu 177 vipivotide tetraxetan) was approved for late-line mCRPC (6), which clinically validated PSMA as a therapeutic target for prostate cancer. PSMA internalizes upon antibody binding (7), making it an ideal target for antibody–drug conjugates (ADC) that deliver cytotoxic drugs to tumor cells via binding to target antigens on tumor cells, internalization, and subsequent release of cytotoxic payload to the cytoplasm. PSMA-targeted ADCs using different payloads and linker technologies have been developed and evaluated in clinical trials. However, all have been discontinued because of ADC instability, leading to dose-limiting toxicities (DLT) and/or lack of efficacy (8–11).

Ambrx utilizes an expanded genetic code technology platform in industry standard cell lines for the incorporation of synthetic amino acid (SAA) into proteins at selected sites. SAAs provide for site-specific, homogeneous, and stable conjugation, overcoming the limitations of traditional conjugation technologies, thereby creating engineered precision biologics. We describe the generation and preclinical characterization of ARX517, a next-generation anti-PSMA ADC optimized for stability and cytotoxic drug delivery efficiency. Key design elements for ARX517 include (i) stable oxime conjugation chemistry (12) to reduce systemic premature payload release and ensure full payload delivery to tumor cells; (ii) site-specific conjugation to SAA to achieve a homogeneous drug-to-antibody ratio (DAR) of 2; (iii) noncleavable polyethylene glycol linker to ensure stability in circulation; and (iv) cell-impermeable

Ambrx, Inc., La Jolla, California.

L.K. Skidmore and D. Mills are co-first authors to this article.

Corresponding Author: Shawn Shao-Hui Zhang, Ambrx, Inc., 10975 North Torrey Pines Road, La Jolla, CA 92037. E-mail: shawn.zhang@ambrx.com

Mol Cancer Ther 2024;XX:XX–XX

doi: 10.1158/1535-7163.MCT-23-0927

payload which is not a substrate for multidrug resistance (MDR) pumps. Engineered for improved stability, ARX517 potentially addresses issues encountered by other anti-PSMA ADCs, such as premature release of toxic payloads, and can maximize efficacy with a fully loaded ADC delivered to target tumor cells and thus widen the therapeutic index (13).

Materials and Methods

Antibody humanization

Humanization of parental mouse anti–PSMA J591 mAb) was performed by grafting mouse heavy chain (HC) and light chain (LC) complementarity-determining regions (CDR) (HC-CDR1:31-35, HC-CDR2:50-66, and HC-CDR3:99-104; LC-CDR1:24-34, LC-CDR2:50-56, and LC-CDR3:89-97) onto different human frameworks selected for the highest homology to the mouse framework sequences and cloning into human IgG1/κ constant regions as a backbone (14). Multiple humanized mAb variants were generated, by pairing four human HC variants with six LC variants, using transient expression in HEK293 cells. Key back mutations were added to the LC framework region to retain binding activity of the antibody. To select the lead clone [Example 2, Table 4 in (14)], the mAb variant supernatants were tested for binding to PSMA-positive LNCaP cells by flow cytometry.

PSMA species cross-reactivity binding by biolayer interferometry

The binding of humanized J591 mAb or ARX517 to human, cyno, and rat PSMA/FOLH1 was measured in a biolayer interferometry assay on an Octet RED96 system (Sartorius). Anti–human IgG Fc capture biosensors (Sartorius) were loaded with purified ARX517 mAb or ARX517 in HEPES buffered saline with surfactant P20 (HBS-P^+) Buffer (Cytiva). After washing biosensors with HBS-P^+ buffer to remove unbound protein, serially diluted PSMA/FOLH1 (human, cyno, or rat) in HBS-P^+ buffer was monitored for association and dissociation kinetics with ARX517 mAb–loaded or ARX517-loaded biosensors. Data were referenced using a parallel buffer blank subtraction. The processed binding curves were globally fitted using the Langmuir model describing a 1:1 binding stoichiometry.

Purification of ARX517 mAb

Clarified cell culture fluid with ARX517 mAb containing SAA para-acetyl-L-phenylalanine was loaded over protein A column (MabSelect SuRe, Cytiva) equilibrated in 25 mmol/L sodium phosphate and 100 mmol/L sodium chloride, pH 7.3. After loading, the column was washed with wash buffer I (20 mmol/L sodium phosphate and 100 mmol/L sodium chloride, pH 7.5) followed by wash buffer II (50 mmol/L sodium acetate, pH 5.5) to remove host cell contaminants. ARX517 mAb was eluted from the column with elution buffer (50 mmol/L sodium acetate, pH 3.4), pooled, and pH-adjusted to pH 5.5 with 1.0 mol/L tris base. The mAb was further purified by loading over a cation exchange column (Capto SP ImpRes, Cytiva) equilibrated in 50 mmol/L sodium acetate, pH 5.5. After loading, the column was washed with wash buffer (50 mmol/L sodium acetate, pH 5.5), and ARX517 mAb was eluted from the column using a linear gradient over 20 column volumes to 100% elution buffer (50 mmol/L sodium acetate and 0.5 mol/L sodium chloride, pH 5.5) and pooled. The cation exchange pool was buffer-exchanged into formulation buffer (20 mmol/L L-histidine and 2.5% trehalose, pH 6.0), concentrated to 40 mg/mL, filtered through a 0.22-μm filter, and stored at ≤−60°C.

Conjugation of ARX517 mAb with AS269

Acetohydrazide catalyst (Sigma) and AS269 drug-linker were added to the ARX517 mAb at a molar excess of 300:1 and 10:1, respectively. The reaction mixture pH was adjusted to 4.0 with 2.0 mol/L acetic acid followed by a water dilution to a final ARX517 mAb concentration of 30 mg/mL. The reaction was incubated at 28°C for 24 hours and then buffer-exchanged by ultrafiltration and diafiltration into formulation buffer to remove excess reagents. The subsequent ARX517 ADC was filtered through a 0.22-μm filter and stored at ≤−60°C.

Peptide mapping

Peptide maps of ARX517 mAb and ADC were obtained using a reverse-phase high-performance liquid chromatography (HPLC) method with mass spectrometric detection. Approximately 200 μg of samples were denatured in Tris-buffered 6 mol/L GdHCl pH 8 and reduced in 20 mmol/L dithiothreitol (DTT) by heating at 37°C for 30 minutes. The samples were allowed to cool to room temperature, and the reduced thiols were alkylated by incubation in 45 mmol/L iodoacetamide in the dark for 30 minutes. The samples were then buffer-exchanged using 0.5 mL Amicon Ultra 10-KDa MWCO spin filters into trypsin digestion buffer containing 50 mmol/L Tris-HCl pH 8. Sequencing Grade Modified Trypsin (Promega) was then added, and the samples were incubated at 37°C for 4 hours. To stop the reaction, 15 μL of 20% trifluoroacetic acid was added to each sample. Thereafter, 20 μL volume of each sample was injected into a 2 × 250 mm Phenomenex Jupiter Proteo 90Å (4 μm) column, and the peptides were separated using a gradient of trifluoroacetic acid and acetonitrile at a flow rate of 0.3 mL/minute. A Thermo Q Exactive Plus mass spectrometer was used to acquire higher-energy collisional dissociation (HCD) tandem mass spectrometric data on top 10 peaks per mass spectrometric scan. The raw data were analyzed using Thermo PepFinder software, and the identities of the peptides were verified manually thereafter.

Hydrophobic interaction chromatography HPLC

The hydrophobic interaction chromatography method was applied to determine the DAR of ARX517 batches. About 50 μg of each sample was loaded on a MAbPac HIC-Butyl HPLC column (Thermo Fisher Scientific) and eluted using a gradient of ammonium sulfate in a phosphate-buffered mobile phase at 0.5 mL/minute. The DAR was calculated using the following equation:

$$DAR = \frac{\sum d^i \star i}{100}$$

in which d^i is the % peak area of the ADC with a drug load of i.

(e.g., 10% total peak area × 1 drug + 90% total peak area × 2 drug = DAR 1.9).

Size-exclusion HPLC

Size variants present in ARX517 were analyzed by size-exclusion chromatography on a TSKgel G3000SWXL column (Tosoh) using an Agilent 1200 series HPLC system with UV detection at 280 nm. Samples were injected at 50 μg load, and separation was achieved by an isocratic elution using a mobile phase consisting of 200 mmol/L potassium phosphate and 250 mmol/L potassium chloride, pH 6.0 at a flow rate of 0.5 mL/minute and column temperature set at 25°C. The percent area of high-molecular weight, monomer, and low-

molecular weight species was calculated using Agilent ChemStation Software.

Differential scanning calorimetry

The thermal transition temperature of ARX517 (diluted to 1 mg/mL using formulation buffer) was determined using a MicroCal capillary VP differential scanning calorimeter. The sample and reference cells were loaded with sample and formulation buffers, respectively. The instrument was programmed to scan from 10°C to 110°C at a rate of 1°C/minute, with a 10-second data averaging period and 15-minute equilibration time. Buffer versus buffer scans were recorded throughout the experiment sequence to obtain a baseline scan to subtract from the experimental data and to ensure the shapes of the baseline scans were reproducible over the course of the experiment. The raw data were processed using MicroCal PEAQ-DSC software to calculate T_m values.

Cell proliferation assay

Prostate cancer cell lines including LNCaP (clone FGC, Cat. # CRL-1740, RRID: CVCL_1379), MDA-PCa-2b (Cat. # CRL-2422, RRID: CVCL_4748), 22Rv1 (Cat. # CRL-2505, RRID: CVCL_1045), and PC-3 (Cat. # CRL-1435, RRID: CVCL_0035) were purchased from ATCC and cultured in the recommended media. C4-2 cells (RRID: CVCL_4782) were purchased directly from MD Anderson Cancer Center and cultured in RPMI 1640 media supplemented with 10% FBS and 100 U/mL penicillin/streptomycin. MDA-PCa-2b cells were initially propagated in male nu/nu mice (Charles River Laboratories), isolated, and then maintained in F-12 K medium supplemented with 20% FBS, 100 U/mL penicillin/streptomycin, 25 ng/mL cholera toxin, 10 ng/mL mouse EGF, 5 μmol/L phosphoethanolamine, 100 pg/mL hydrocortisone, 45 nmol/L sodium selenite, and 5 μg/mL human recombinant insulin as recommended by ATCC. All cell lines were used in the *in vitro* assays within 1 month after thawing the frozen vial. Cell line authentication and *Mycoplasma* testing were not conducted for cell lines purchased from ATCC. The C4-2 cell line was confirmed negative for *Mycoplasma* (by touchdown PCR) after receipt at Ambrx.

Cells were seeded at 3,000 cells/well in 96-well white plates using their respective media and incubated at 37°C and 5% CO_2 overnight. The next day, serially diluted ARX517 or monomethyl auristatin E (MMAE) was added to the cells and incubated at 37°C and 5% CO_2 for 4 days. At the end of incubation, cell viability was measured using CellTiter-Glo 2.0 reagent (Promega) in a SpectraMax M5E luminometer. The IC_{50} value was determined by a 4PL curve fitting using GraphPad Prism software (Version 8.2.1), and the % E_{max} for the dose of 30 nmol/L was calculated by subtracting the % viability from 100%.

PSMA expression level determination

The quantitative determination of PSMA surface expression was performed using QIFIKIT (Agilent Dako, part number K007811-8) according to the manufacturer's recommendations. Each cell line was harvested using StemPro Accutase cell dissociation reagent (Gibco, catalog number A1110501) and incubated with mouse anti–human PSMA antibody (BioLegend, catalog #342502, clone LNI-17), isotype control antibody (BioLegend, catalog number 401401, Clone MGI-45), or FACS buffer only for 1 hour at 4°C. After washing, the cells were incubated with FITC-conjugated anti-mouse secondary antibody, along with set up beads and calibration beads, for 45 minutes at 4°C in the dark. Following washing and resuspension of the cells and beads, FITC fluorescence was analyzed using FACSCanto II (BD Biosciences). PSMA receptor numbers were calculated using a lot-specific standard curve obtained from calibration beads.

Mouse pharmacokinetic study design

Male nude (nu/nu) mice (RRID: IMSR_CRL:088) with and without C4-2 tumors were dosed intravenously with ARX517 at 1 or 5 mg/kg ($n = 5$/group). Blood samples were collected from all animals at predose and 0.5, 2, 6, 24, 48, 72, 168, 240, 336, 504, and 672 hours postdose. Blood samples were immediately diluted 10-fold into casein–PBS (Thermo Fisher Scientific, catalog # 37528) and frozen in tubes at −60°C to −80°C. The samples were analyzed in total antibody (TA) and intact ADC bioanalytic assays. Mouse pharmacokinetic (PK) studies were approved by the Institutional Animal Care and Use Committee under protocol ACUP ABX23-01.

Bioanalytic assays in the mouse matrix

An ARX517 TA assay was developed to detect unconjugated and all conjugated antibody species in mouse nu/nu serum. Meso Scale Discovery (MSD) High Bind plates were coated overnight at 4°C with recombinant human PSMA (R&D Systems, catalog # 4234-ZN-010) and then blocked with casein–PBS (Thermo Fisher Scientific, catalog # 37528) for at least 1 hour at room temperature the next day. The plates were washed three times in 1× wash buffer (20× KPL Wash Solution, KPL, catalog # 50-63-04), and ARX517 standard (STD), quality controls (QC), and samples prediluted 1:50 in casein–PBS were added in duplicate to the plates. After incubation for 2 hours at room temperature, MSD plates were washed three times as before, and biotinylated goat anti–human κ detection antibody (SouthernBiotech, catalog # 2061-08) was incubated for 1 hour at room temperature. Following a wash step to remove unbound antibodies, Streptavidin-SULFO tag reagent (MSD, catalog # R32AD-1) was added for 1 hour at room temperature. After a final wash step, 1× Read Buffer T (4× Read Buffer T, MSD, catalog # R92TC-2) was added, and the plates were read in an MSD QuickPlex SQ 120 unit. The lower limit of quantitation (LLOQ) of the assay in nu/nu mouse serum was 39.1 ng/mL.

The ARX517 intact ADC assay in mouse nu/nu serum was designed to only specifically detect ADC with two drug-linkers [not ADC with one drug-linker, unconjugated mAb, or free para-acetylphenylalanine (pAF)-AS269] to enable determination of any loss of AS269 drug-linker when comparing intact ADC curves with TA curves. The assay procedure was similar to the TA assay, except that MSD High Bind plates were coated with AMB-20, an anti–AS269-specific rabbit mAb), and the detection antibody was biotinylated-AMB-20. The LLOQ of the intact ADC assay in nu/nu mouse serum was 125 ng/mL.

PK parameters for TA and intact ADC data were analyzed in Phoenix WinNonlin software (Certara), using noncompartmental analysis. A minimum of three time points were required for the determination of the elimination rate constant, upon which disposition parameters were calculated. Concentrations that were below the limit of quantitation were set to zero for PK analysis.

Ex vivo human serum stability assay

ARX517 was diluted to 200 μg/mL in pooled human serum (Bioreclamation, catalog # HMNSRM), and 100 μL aliquots in sterile 0.6-mL Eppendorf tubes were incubated upright in an incubator set to 37°C, under 5% CO_2 for 21 days. Individual tubes were removed after 0, 1, 4, 6, 8, 11, 14, and 21 days of incubation and frozen in an −80°C freezer until all time points were collected.

All samples were diluted to 500 ng/mL in human serum to fall within the quantitative range of the PK assays and analyzed in duplicate in TA and intact ADC assays using the MSD platform. The TA and intact ADC assays in human serum used the same reagents for capture and detection as the mouse TA and intact ADC assays. The LLOQ values of the TA and intact ADC assays in human serum were 65.3 and 32.7 ng/mL, respectively.

Cell line–derived xenograft and patient-derived xenograft models

C4-2 and MDA-PCa-2b cells (described in "Cell proliferation assay") were grown to near confluency. Freshly harvested cells were suspended in PBS and mixed 1:1 with Matrigel. NCG (RRID: IMSR_CRL:572) or nu/nu mice were anesthetized with isoflurane (2%–3%, 2 L/minutes oxygen) and implanted subcutaneously in the right flank with 5×10^6 cells/mouse in 0.2 mL cell suspension. NOD/SCIDγ mice (RRID: IMSR_JAX:005557) containing subcutaneously implanted TM00298 patient-derived xenograft (PDX) cells were obtained from The Jackson Laboratory. For CTG-2440 studies (Champions Oncology), NOG mice (RRID: IMSR_TAC:HSCFTL-NOG) were subcutaneously implanted with fragments derived from 1,000 to 1,500 mm^3 donor mouse tumors.

Twice weekly, the body weight was recorded, and both tumor length and width were measured using electronic calipers. Tumor volume (TV) was calculated as $L \times W \times W \times 0.5$ (in which L is the tumor length and W is the tumor width). When TV equaled 150 to 500 mm^3, mice were randomized into approximately equal TV average groups and dosed intravenously at 10 mL/kg with vehicle or the indicated test articles. Enzalutamide was administered orally at 10 mg/kg in 1% carboxymethyl cellulose and 0.1% Tween-80. Percent tumor growth inhibition (% TGI) was calculated as $100 \times [1-$(TV or wet weight of the treatment group/TV or wet weight of the control group)]. Mouse pharmacology studies were executed in compliance with institutional guidelines and regulations and after Institutional Animal Care and Use Committee approval under protocol ACUP ABX22-01.

Toxicology study designs

Male and female Sprague–Dawley rats (7–10 weeks old) were dosed with vehicle ($n = 3$/sex/group) or ARX517 (20, 40, or 60 mg/kg, $n = 6$/sex/group) via intravenous infusion over approximately 20 minutes at a dose volume of 15 mL/kg. Following test article administration, rats were observed for 28 days and necropsied on day 29. Toxicologic observations/evaluations were all performed using standard methodology and included mortality, clinical observations, injection site observation, body weight, food consumption, safety pharmacology examinations (functional observational battery test and respiration examination), clinical pathology (hematology, coagulation, serum chemistry, and urinalysis), gross observations, terminal necropsy organ weights, and histopathologic evaluation. At various time points after dosing, jugular vein blood samples were collected for clinical pathology. For histopathology, all major tissues were trimmed and fixed in 10% neutral-buffered formalin, except for eyes with optic nerves, testes, and epididymides, which were fixed in modified Davidson's solution for 24 to 72 hours. Preserved tissues were embedded in paraffin, sectioned, stained with hematoxylin and eosin, and examined microscopically by a licensed pathologist.

Male and female cynomolgus monkeys (2.5–3.5 years old, $n = 6$/sex/group) were dosed twice, 3 weeks apart, with vehicle or ARX517 (1, 6, or 9 mg/kg) via intravenous infusion over approximately 20 minutes at a dose volume of 5 mL/kg. Four monkeys/sex in each group were euthanized and necropsied 1 week after the final ARX517 dose, and the remaining two animals/sex (recovery group) were observed for another 6 weeks, followed by terminal necropsy. Toxicologic assessments were performed as described above.

Cynomolgus monkey toxicokinetic and antidrug antibody assays

To determine serum concentrations of ARX517 TA, ADC, and payload pAF-AS269, blood samples were collected from all available study animals at 0 (predose); at 0.5, 4, 8, 24, 72, 120, 168, 336, and 504 hours after the first ARX517 dose; and at 0.5, 4, 8, 24, 72, 120, and 168 hours (dosing phase) and 336, 504, 672, 840, and 1176 hours (recovery phase) after the second ARX517 dose. Blood samples were processed to serum, aliquoted, and stored in a freezer set to ≤−65°C.

The samples were analyzed in validated PK assays. The TA PK assay in cynomolgus monkey serum used the same capture and detection reagents as the TA assay in the mouse matrix. The ADC PK assay in cynomolgus serum was similar to the intact ADC assay in the mouse matrix except that the MSD High Bind plates were coated with recombinant human PSMA. The LLOQ values of the TA and ADC assays in cynomolgus serum were 78.1 and 19.5 ng/mL, respectively. To extract pAF-AS269 from 30 μL of study samples, STDs, and QCs, a protein precipitation step was performed with 200 ng/mL internal standard (diclofenac) and 190 μL of 0.1% formic acid in acetonitrile in a 96-well, deep-well plate. Samples, STDs, and QCs were vortexed for 10 minutes and centrifuged at $3{,}220 \times g$ for 15 minutes at 4°C, and 100 μL supernatant was transferred to a new 96-well, deep-well plate. Deionized water (100 μL) was added to the transferred supernatants, vortexed for 5 minutes, and centrifuged at $3{,}220 \times g$ for 5 minutes at 4°C. The extracted samples (10 μL) were injected into an LC/MS-MS system for chromatographic separation and detection with the positive ion ESI mode. The LLOQ of the pAF-AS269 assay in cynomolgus serum was 0.2 ng/mL.

Toxicokinetic (TK) parameters for TA and ADC were calculated using serum concentrations and noncompartmental analysis using Phoenix WinNonlin software (Certara).

Samples collected from animals on day 1 (cycle 1 predose), day 22 (cycle 2 predose), day 29 (168 hours after the second ARX517 dose), and at the end of the recovery phase (1,176 hours after the second ARX517 dose) were processed to serum and evaluated for immunogenicity response using a validated ARX517 antidrug antibody (ADA) assay. The ADA screening assay mean sensitivity was established as 8.2 ng/mL in neat serum; assay drug tolerance was 100 μg/mL ARX517 for 500 ng/mL positive control ADA and 20 μg/mL ARX517 for 100 ng/mL positive control ADA.

Data availability

Data were generated by the authors and available on request.

Results

ARX517 displays high-affinity target binding, high thermal stability, and homogeneous DAR

The murine mAb J591 has been previously described elsewhere and binds the extracellular domain of human PSMA with high affinity (15, 16). The selection of the final humanized J591 (huJ591) mAb candidate was based on successful retention of human PSMA binding activity and the lowest number of back mutations required

to maintain binding affinity (14). Evaluation of huJ591 mAb in a cross-species PSMA biolayer interferometry binding assay showed similar high-affinity binding to human and cynomolgus monkey PSMA (apparent K_D values were 0.62 and 0.79 nmol/L, respectively) and no binding to rat PSMA (**Fig. 1A**).

Next, we generated an ADC by site-specifically conjugating drug-linker AS269 (17), a highly potent microtubule inhibitor belonging to the auristatin class of drugs, to the SAA pAF incorporated at HC position alanine 114 (HA114, by Kabat numbering) in the huJ591 mAb. The aminooxy group of AS269 reacts with the ketone group of pAF to form a stable oxime bond (**Fig. 1B**). The ADC, named ARX517, bound human and cynomolgus monkey PSMA with similar affinities as the huJ591 mAb (and did not bind rat PSMA), confirming that the conjugation of AS269 at site HA114 did not impact binding activity of the ADC (**Fig. 1A**).

ARX517 evaluation by mass spectrometry analysis confirmed that AS269 conjugation only occurred at the HA114 site, with the HC peptide HC:101-119 shifting to the theoretical conjugate retention time in the ADC peptide map chromatogram (**Fig. 2A**). The HIC-HPLC assay confirmed an average DAR of 1.9, with mostly DAR2 species, minimal DAR1 species, and no unconjugated mAb observed (**Fig. 2B**). ARX517 exhibited high purity (98% main peak) and minimal aggregation (1.7% high molecular weight species) from the size-exclusion chromatography HPLC data (**Fig. 2C**). Additional analytic characterization by differential scanning calorimetry showed minimal impact of conjugation on the thermodynamic stability of ARX517, with no detectable differences in overall conformation between mAb and ADC lots (**Fig. 2D**).

ARX517 promotes *in vitro* cytotoxicity of PSMA-expressing tumor cell lines

We quantified PSMA cell surface expression levels in multiple prostate cancer cell lines using QIFIKIT and determined expression ranged from <1,000 to 136,000 receptors per cell. Treatment of cell lines with ARX517 in 4-day cellular proliferation assays resulted in potent subnanomolar activity (IC_{50} values ≤0.5 nmol/L) and high maximum efficacy of ARX517 in cells expressing moderate-to-high PSMA levels (MDA-PCa-2b, LNCaP, and C4-2; **Table 1**). Minimal ARX517 activity was observed in cell lines with very low or no PSMA expression (22Rv1 and PC-3), demonstrating the selectivity of ARX517, which requires expression of PSMA for activity (**Fig. 1C**). All tested cell lines were sensitive to the auristatin class of drugs as the positive control MMAE strongly inhibited proliferation in a similar manner across all tested cell lines with IC_{50} values ranging from 0.18 to 0.78 nmol/L (**Table 1**).

ARX517 demonstrates stability in mouse PK and *ex vivo* human serum studies

To assess the *in vivo* stability and PK of ARX517, male nu/nu mice bearing C4-2 prostate tumors or no tumors were administered a single intravenous dose of ARX517 at 1 or 5 mg/kg to cover a range of efficacious doses in pharmacology models. Blood samples were analyzed in qualified ligand-binding assays designed to measure TA (unconjugated and conjugated antibody species) and intact ADC (ADC species with two drug-linkers only). A comparison of the TA and intact ADC concentration–time curves enables stringent detection of any loss of drug-linker AS269. ARX517 exhibited overlapping TA and intact ADC concentration–time curves at both dose levels (**Fig. 3A** and **B**) with the mean AUC from time zero to last quantifiable concentration (AUC_{0-last}) ratios from 1.07 to 1.23, indicating that deconjugation of drug-linker is not observed and ARX517 was stable in circulation for the duration of the 28-day study (**Table 2**). The resulting ADC terminal half-life ($t_{1/2}$) was long in mice with no tumors (mean $t_{1/2}$ ranged from 261 to 350 hours) and in mice bearing tumors (mean $t_{1/2}$ ranged from 210 to 237 hours). The $t_{1/2}$ seemed slightly shorter for tumor-bearing mice, but the difference may fall within the variability of the study (**Table 2**).

Subsequently, we extended our evaluation of ARX517 stability to an *ex vivo* human serum assay. ARX517 diluted to 200 μg/mL in human serum was incubated in aliquots at 37°C under 5% CO_2 for 21 days with samples collected at different time points and analyzed in ARX517 TA and intact ADC assays to assess stability. The TA and intact ADC concentrations at all time points were highly similar, with ADC versus TA ratios ranging from 0.91 to 1.16 (Supplementary Table S1). The percent differences from theoretical values for TA and intact ADC were all within 30% difference, which was considered within assay variability. Overall, the data demonstrated that ARX517 is stable in human serum under the tested assay conditions for 21 days.

ARX517 controls tumor growth in enzalutamide-sensitive and -resistant models

We next evaluated the ability of ARX517 to control tumor growth in a series of *in vivo* cell line–derived xenograft and PDX models. In these studies, ARX517 did not induce severe body weight loss, mortality, or morbidity. In an initial study in mice with subcutaneously implanted PSMA-expressing MDA-PCa-2b tumors, a single intravenous ARX517 administration demonstrated robust TGI up to 83% (at the 5 and 10 mg/kg doses), whereas 10 mg/kg unconjugated mAb or isotype control ADC (containing AS269) did not inhibit tumor growth (**Fig. 4A**).

Moreover, in the enzalutamide-sensitive TM00298 PCa PDX model, once weekly ARX517 administration inhibited tumor growth in a dose-dependent manner (up to 66% in the 3 mg/kg group; $P < 0.0001$ vs. vehicle), and daily enzalutamide administration (10 mg/kg) induced 41% TGI ($P < 0.01$). In this TM00298 model, ARX517 and enzalutamide combination resulted in additive efficacy, with a TGI of 85% ($P < 0.0001$; **Fig. 4B**). In a second PDX prostate cancer model, CTG-2440, once weekly administration of ARX517 as a single agent inhibited tumor growth in a dose-dependent manner up to 92%. At 3 mg/kg in this model, ARX517 induced more robust TGI than 10 mg/kg enzalutamide (92% vs. 38%, respectively; **Fig. 4C**).

Because most patients with prostate cancer eventually progress to androgen deprivation therapy–resistant disease, we evaluated ARX517 activity in the enzalutamide-resistant C4-2 cell line–derived xenograft model. Encouragingly, ARX517 promoted C4-2 TGI after a single dose as low as 1 mg/kg, and progression-free disease was observed after a single dose of 5.0 mg/kg (**Fig. 4D**). Once weekly ARX517 administration resulted in 37% (1 mg/kg) to 79% (3 mg/kg) TGI in the C4-2 model. Consistent with C4-2 enzalutamide resistance, the combination of ARX517 and enzalutamide (10 mg/kg) did not lead to additive TGI (**Fig. 4E**).

ARX517 demonstrated robust efficacy in these pharmacology models, and importantly, ARX517 efficacy was always greater than that of enzalutamide which is a standard-of-care and important treatment for patients with prostate cancer. In summary, ARX517 inhibited tumor growth in multiple enzalutamide-sensitive and -resistant xenograft models and produced additive efficacy with enzalutamide in an enzalutamide-sensitive tumor model.

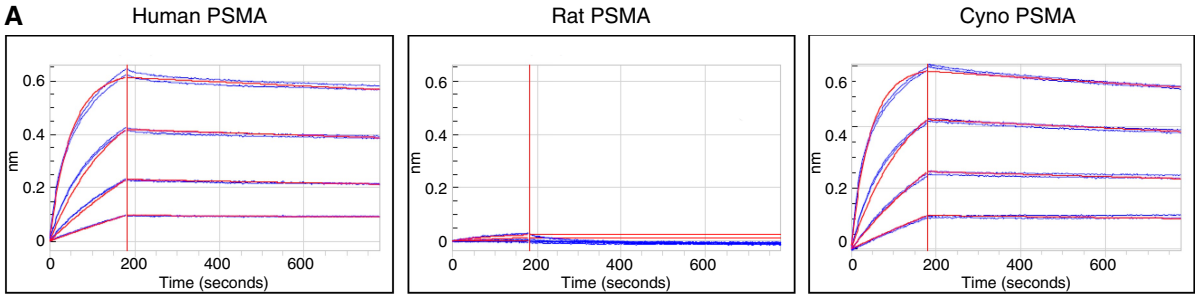

Analyte	Human K_D (M)	Rat K_D (M)	Cyno K_D (M)
huJ591 mAb	6.23 E-10	No binding	7.9 E-10
ARX517	5.04 E-10	No binding	6.81 E-10

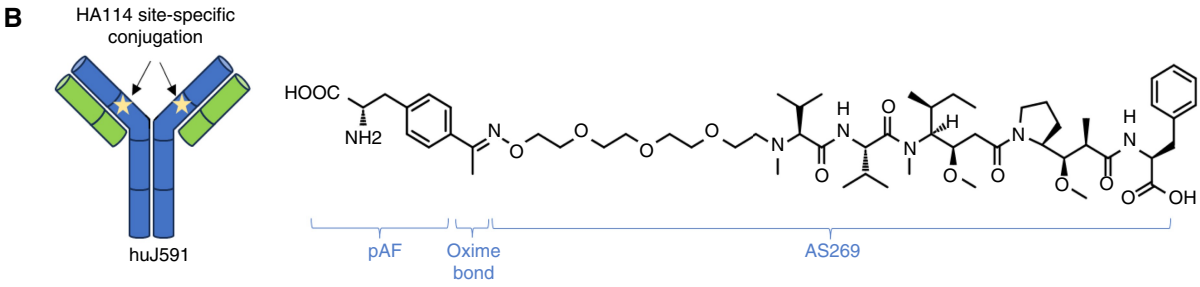

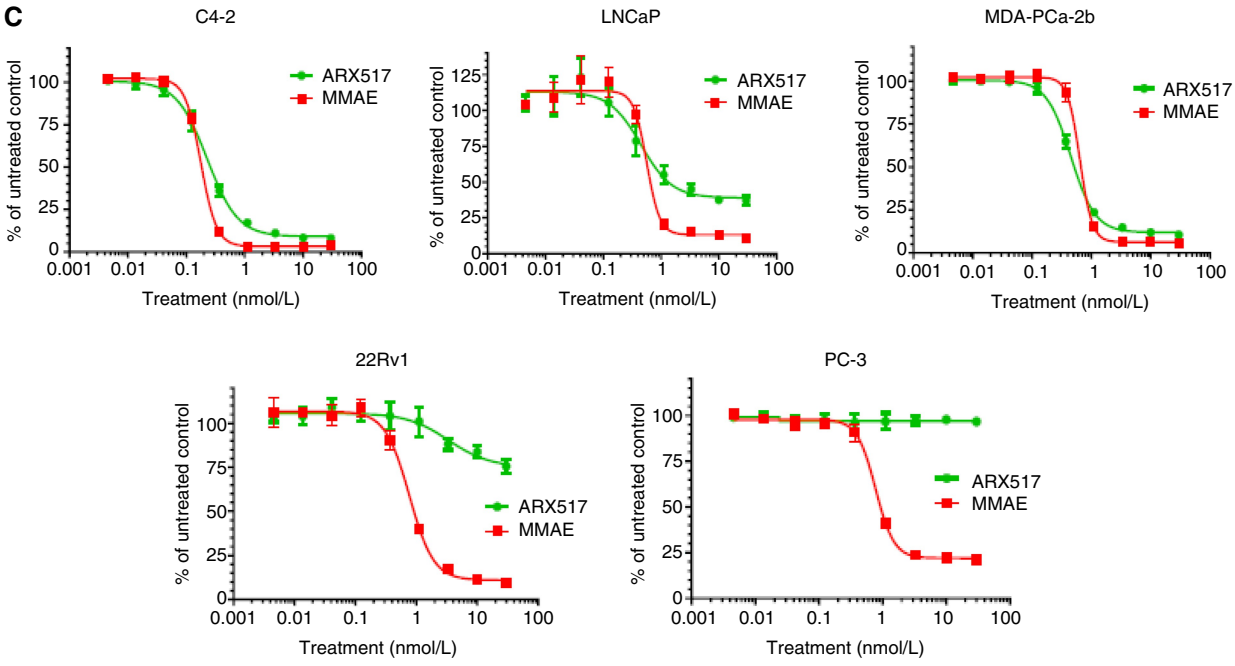

Figure 1.

ARX517 binds comparably to human and cynomolgus monkey PSMA and exhibits robust *in vitro* cytotoxicity in PSMA-expressing lines. **A,** huJ591 mAb or ARX517 was immobilized onto biosensors, and association/dissociation with serially diluted PSMA from the indicated species was measured via biolayer interferometry. Sensorgram traces for huJ591 mAb are shown. Affinities were calculated from PSMA binding curves that were globally fitted using a 1:1 stoichiometry binding model. **B,** Schematic representation of ARX517 in which drug-linker AS269 is conjugated via a stable oxime bond to the pAF residues incorporated at the HC ALA114 site in the huJ591 mAb. **C,** Dose–response curves show relative cell viability (% of untreated control samples) in cells treated for 4 days with serially diluted ARX517 or a positive control, cell-permeable auristatin, MMAE.

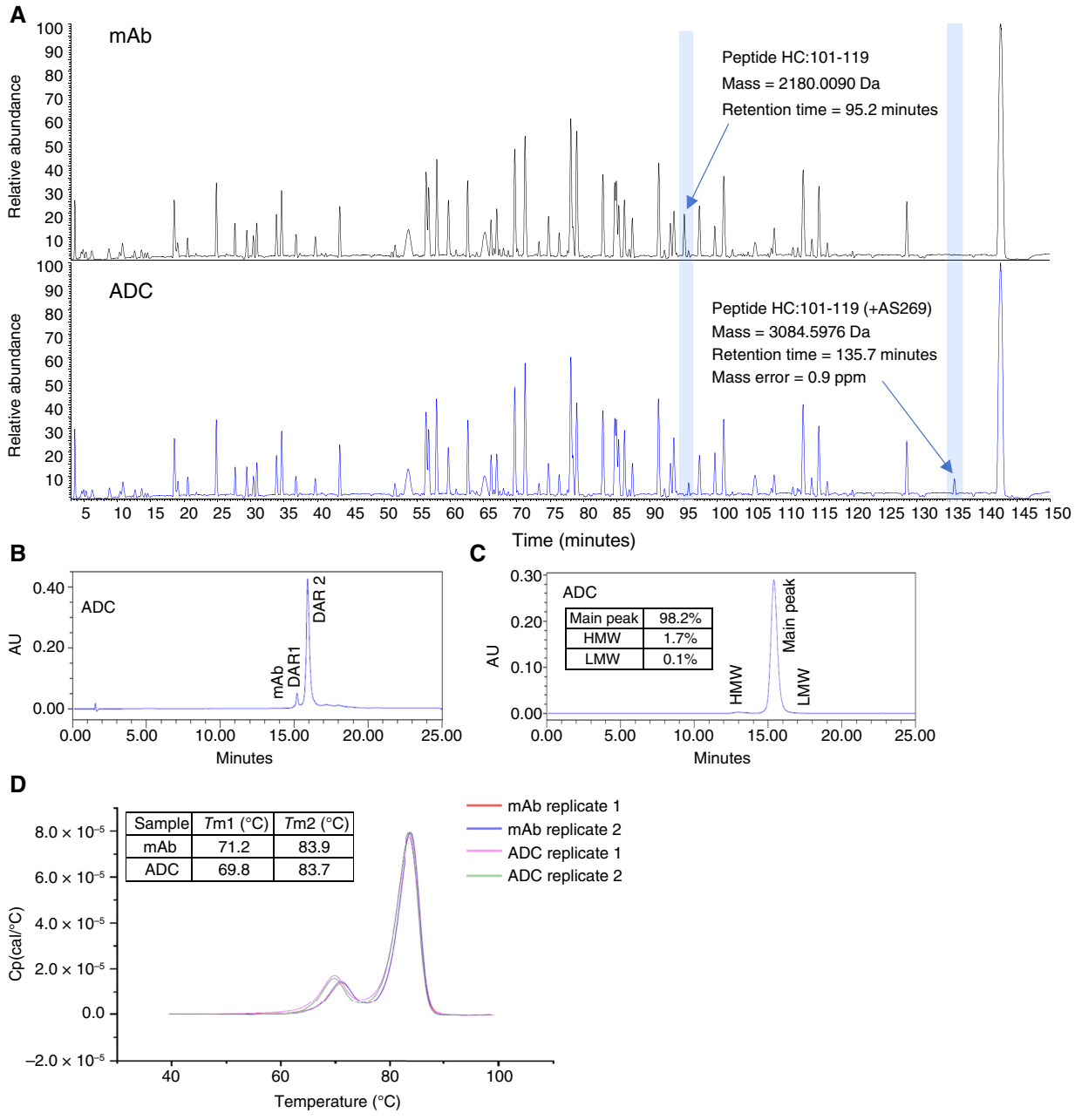

Figure 2.

Analytic characterization of the ARX517 confirmed site of AS269 conjugation, controlled DAR), high purity with minimal aggregation, and high thermal stability postconjugation. **A,** Peptide maps of unconjugated mAb and ARX517 using the reverse-phase HPLC method with mass spectrometric detection are shown. **B,** HIC method with UV detection at 280 nm resolved ARX517 unconjugated mAb, DAR1, and DAR2 species. **C,** Size exclusion chromatography HPLC with UV detection at 280 nm quantified ARX517 size variants. The percent area of high molecular weight, monomer, and low molecular weight species were calculated using Agilent ChemStation software. **D,** The T_m values of unconjugated mAb and ARX517 were determined using a differential scanning calorimeter. HMW, high molecular weight; LMW, low molecular weight.

ARX517 exhibits favorable tolerability and TK profiles

ARX517 was evaluated in a single-dose Good Laboratory Practice toxicity study in Sprague–Dawley rats and a Good Laboratory Practice repeat-dose toxicity study in cynomolgus monkeys. Because it does not bind rodent PSMA, the rat study findings reveal ARX517's acute target-independent toxicologic profile. The administration of a single ARX517 dose to rats over a 20-minute intravenous infusion at 20, 40, or 60 mg/kg did not result in treatment-related mortality, moribundity, abnormalities in behavioral testing, or respiratory findings. At day 4 postinfusion, clinical pathology findings included increased neutrophil and monocyte counts, reduced lymphocyte counts, decreased red blood cell (RBC)

Table 1. ARX517 and MMAE *in vitro* potency (IC_{50}) and maximum efficacy (E_{max}) in prostate cancer cell lines.

Cell line	PSMA surface number (QIFIKIT)	ARX517 IC_{50} (nmol/L)	ARX517 E_{max} (%)	MMAE IC_{50} (nmol/L)	MMAE E_{max} (%)
C4-2	87,000	0.228	92	0.178	96
LNCaP	136,000	0.449	63	0.566	89
MDA-PCa-2b	46,000	0.451	89	0.641	94
22Rv1	6,000	3.366	24	0.771	91
PC-3	<1,000	>30	3	0.778	79

parameters [RBC/hemoglobin/hematocrit (HCT)], and changes in hepatic function [increased aspartate aminotransferase (AST)/alanine aminotransferase (ALT)/alkaline phosphatase (ALP)/total bilirubin (TBIL)] and renal function [increased creatinine (CRE)] at doses ≥40 mg/kg. Both sexes had significant test article–related weight increases in the liver, spleen, and lungs. At the end of a 28-day observation period, ARX517-related histopathologic adverse findings were observed in male reproductive organs and the lungs of both sexes at doses ≥20 mg/kg, and the MTD was 60 mg/kg.

Because it binds to cynomolgus monkey and human PSMA with similar affinity, we evaluated ARX517 on-target and off-target toxicologic profiles in cynomolgus monkeys following two intravenous administrations of 1, 6, or 9 mg/kg given 3 weeks apart. In this study, the ARX517 no observed adverse effect level (NOAEL) was 1 mg/kg/dose and the highest non-severely toxic dose (HNSTD) was 6 mg/kg/dose for both male and female monkeys. At day 6 following the second ARX517 dose, clinical pathology findings were all considered nonadverse, were only observed at doses ≥6 mg/kg, and included increased monocyte counts, reduced platelet counts, increased coagulation time [activated partial thromboplastin time (APTT)], and increased hepatocellular enzymes [AST/ALP/gamma-glutamyl transferase (GGT)]. At the HNSTD, although histopathologic target organs included the liver, spleen, and thymus, all adverse findings had normalized and were reduced in incidence/severity at the end of the 6-week recovery period. At the 9 mg/kg dose (above the HNSTD), additional target organs were kidney and mild lung findings in one monkey. Importantly, no ophthalmologic, respiratory, urinary, cardiovascular, or neurologic findings were observed at any dose.

The ARX517 toxicokinetic profile in the cynomolgus repeat-dose study showed stability of ARX517 in the systemic circulation, with overlapping TA and ADC concentration–time curves at all doses (**Fig. 3C**).

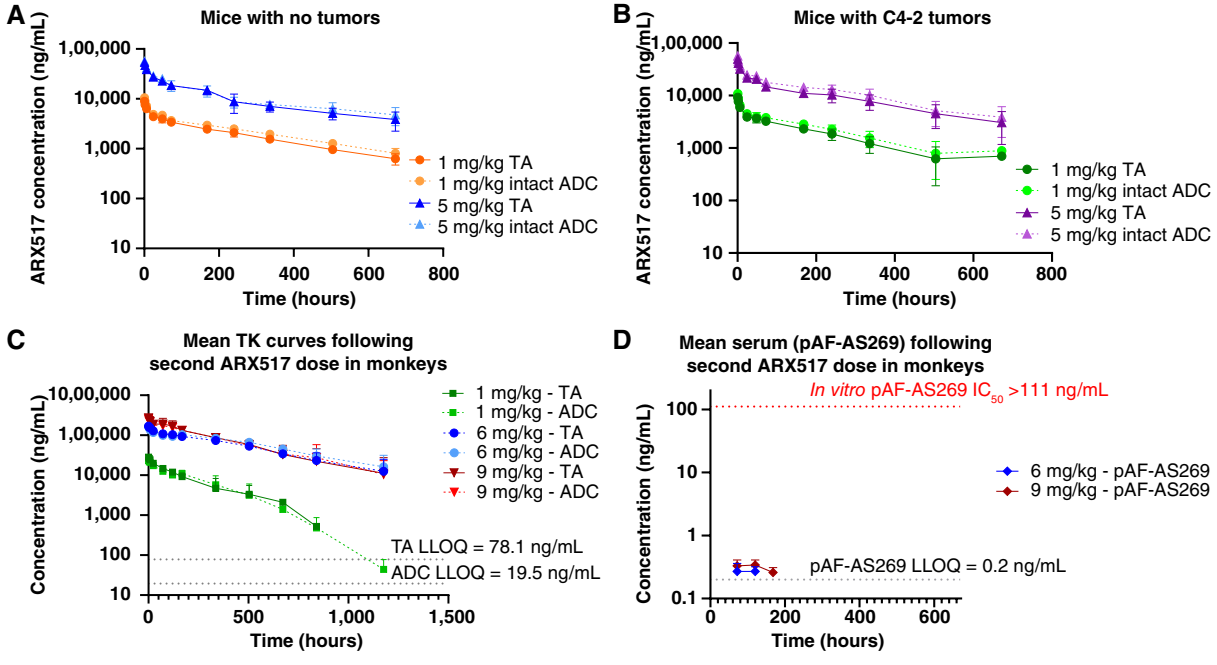

Figure 3.

Linear PK and prolonged stability with minimal payload release following ARX517 dosing in mice and cynomolgus monkeys. nu/nu mice (**A**) without and (**B**) with C4-2 tumors ($n = 5$ mice/group) were dosed intravenously with ARX517. Blood samples were collected at the indicated time points and analyzed in qualified TA and intact ADC bioanalytic assays. Blood samples were collected from cynomolgus monkeys ($n = 6$/sex/group) following ARX517 dosing. **C,** TA, ADC, and (**D**) pAF-AS269 serum concentrations were quantified using validated assays (see "Materials and Methods"). Shown are mean ± SD (upper error bars) for TA, ADC, and pAF-AS269 (time points with $n \geq 5$ quantifiable concentrations).

Table 2. ARX517 PK parameters in mice ± tumors.

Mice	Dose (mg/kg)	Analyte	C_{max} (ng/mL)	AUC_{last} (hour × ng/mL)	$t_{1/2}$ (hours)	ADC vs. TA AUC_{last} ratio	Tumor-bearing vs. no tumor AUC_{last} ratio	Tumor-bearing vs. no tumor $t_{1/2}$ ratio
No tumor ($n = 5$)	1	TA	8,950	1,290,000	242	NA	NA	NA
		ADC	10,500	1,550,000	261	1.20	NA	NA
	5	TA	53,900	6,920,000	290	NA	NA	NA
		ADC	57,000	7,380,000	350	1.07	NA	NA
C4-2 tumor–bearing ($n = 5$)	1	TA	9,240	1,110,000	211	NA	0.86	0.87
		ADC	10,800	1,330,000	210	1.20	0.86	0.80
	5	TA	49,500	6,160,000	242	NA	0.89	0.83
		ADC	57,100	7,570,000	237	1.23	1.03	0.68

Mean PK parameters for TA and ADC assays were analyzed using noncompartmental analysis for all dose groups ($n = 5$ mice/group).

ARX517 TA versus ADC exposure was similar with mean maximum observed concentration (C_{max}) and AUC_{last} ratios within 0.77 to 1.07 (**Table 3**). After administration of the second dose of ARX517, released payload pAF-AS269 was not quantifiable for all animals in the 1 mg/kg dose group and for three animals in the 6 mg/kg dose group. In the remaining animals in the 6 or 9 mg/kg

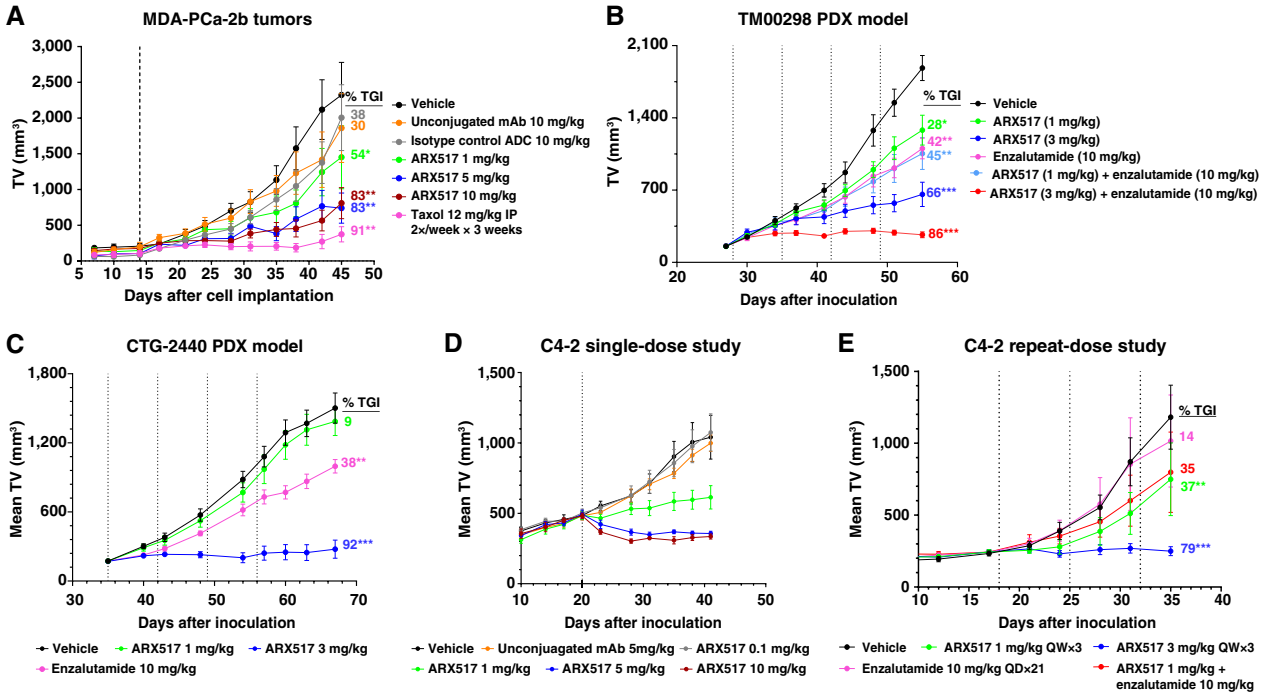

Figure 4.

ARX517 inhibits tumor growth in multiple prostate CDX and PDX models. All graphs show mean TVs ± SEM over time. **A,** In the MDA-PCa-2b murine xenograft model, MDA-PCa-2b cells were implanted subcutaneously into the flank of male nu/nu mice ($n = 10$/group). When tumors reached 100–200 mm^3, mice were given a single intravenous dose of the indicated test articles (dotted line, day 14). % TGI was calculated based on tumor wet weights at day 45 after cell implantation. Statistical analysis: *, $P < 0.05$; **, $P < 0.01$, calculated using the nonparametric Mann–Whitney *t* test. In the enzalutamide-sensitive (**B**) TM00298 and (**C**) CTG-2440 PDX models, mice [(**B**) NOD/SCIDγ mice, $n = 9$/group; (**C**) NOG mice, $n = 10$/group for vehicle and 1 mg/kg ARX517, $n = 9$/group for other cohorts] were subcutaneously implanted with patient-derived tumor cells. When tumors reached 100–200 mm^3, mice were dosed intravenously with ARX517 once weekly for four total doses (dotted lines show ARX517 doses) and/or enzalutamide orally in **B** daily for 28 days or in **C** daily for 5 days, followed by no dosing for 2 days, in a week for 4 weeks. % TGI was calculated based on TV measurements at study end. Statistical analysis: *, $P < 0.05$; **, $P < 0.01$; ***, $P < 0.001$; *P* values were calculated in **B** using nonparametric Mann–Whitney *t* test and in **C** using one-way ANOVA followed by the Tukey multiple comparisons test. **D** and **E,** nu/nu mice (**D**; $n = 10$/group; except $n = 5$ for the ARX517 10 mg/kg group) or NCG mice (**E**; $n = 7$/group for enzalutamide and combination treatment groups; $n = 10$/group for other cohorts) were subcutaneously implanted with enzalutamide-resistant C4-2 tumor cells in Matrigel. When tumors reached 200–500 mm^3, mice were dosed intravenously with the indicated test articles (dotted lines show ARX517 doses). % TGI in **E** was calculated based on TV measurements at study end. Statistical analysis: **, $P < 0.01$; ***, $P < 0.001$ calculated using a two-way ANOVA with repeated measures and Tukey *post hoc* test.

Table 3. ARX517 TK parameters in cynomolgus monkey repeat-dose toxicity study.

Dose (mg/kg)	Sex	Analyte	C_{max} (ng/mL)	T_{max} (hours)[a]	AUC_{0-last} (h × ng/mL)	$t_{1/2}$ (hour)	$AUC_{0-168\ hours}$ (h × ng/mL)	ADC/TA C_{max} ratio	ADC/TA AUC_{last} ratio
1	Male	TA	29,300	0.5	3,110,000	108	2,480,000	NA	NA
		ADC	24,900	0.5	2,870,000	151	2,130,000	0.85	0.92
	Female	TA	27,500	0.5	3,300,000	132	2,570,000	NA	NA
		ADC	23,800	0.5	3,300,000	135	2,350,000	0.87	1.00
6	Male	TA	177,000	0.5	34,600,000	265	19,800,000	NA	NA
		ADC	175,000	0.5	36,500,000	324	18,800,000	0.99	1.05
	Female	TA	168,000	0.5	33,500,000	378	18,000,000	NA	NA
		ADC	152,000	0.5	35,100,000	315	16,500,000	0.90	1.05
9	Male	TA	257,000	0.5	41,400,000	250	27,100,000	NA	NA
		ADC	266,000	0.5	44,100,000	284	29,600,000	1.04	1.07
	Female	TA	316,000	0.5	54,100,000	320	33,700,000	NA	NA
		ADC	243,000	0.5	47,000,000	308	26,500,000	0.77	0.87

Mean TK parameters (median for T_{max}) after the second ARX517 dose were calculated for all dose groups (for $n = 6$ monkeys/sex/group), except in the 6 and 9 mg/kg female dose groups in which one monkey in each group was excluded because of development of ADA.
[a]Median value for T_{max}.

dose groups, pAF-AS269 generally seemed slowly in circulation with a small number of quantifiable time points at low concentrations near the assay LLOQ of 0.2 ng/mL (**Fig. 3D**). These low concentrations of pAF-AS269 are >100-fold lower than the observed *in vitro* activity of pAF-AS269 (IC_{50} >100 nmol/L, or 111 ng/mL). The delayed appearance of pAF-AS269 (median time to C_{max} observed 120 hours after dosing ARX517) in circulation indicates the high stability of the ADC, with minimal extracellular deconjugation. Two female monkeys (one each in the 6 and 9 mg/kg dose groups) were excluded from the TK analyses because of the early development of ADA that impacted TA, ADC, and pAF-AS269 concentrations.

At the HNSTD of 6 mg/kg in male monkeys, the ARX517 AUC_{last}, C_{max}, and $t_{1/2}$ after the second dose were 36,500,000 hours × ng/mL, 175,000 ng/mL, and 324 hours, respectively (**Table 3**). At the pharmacologically active dose of 5 mg/kg in C4-2 tumor–bearing mice, ARX517 mean AUC_{last}, C_{max}, and $t_{1/2}$ were 7,570,000 hours × ng/mL, 57,100 ng/mL, and 237 hours, respectively (**Table 2**). A comparison of ARX517 exposure at the 5 mg/kg dose evaluated in PK studies, which is higher than the pharmacologically active dose of 3 mg/kg observed in multiple models, versus exposure at the HNSTD in monkey toxicology studies shows a clear therapeutic index of fivefold for AUC_{last} and threefold for C_{max}.

Taken together, the pharmacologic, toxicologic, and PK profiles suggest that ARX517 is well tolerated at exposures much higher than those required for efficacy, providing a rationale for clinical investigation as a potential mCRPC treatment option.

Discussion

In this report, we describe the generation and preclinical characterization of ARX517, a PSMA-directed, site-specific, highly stable ADC for mCRPC treatment. ARX517 selectively kills PSMA-high but not PSMA-negative cells *in vitro* and inhibits tumor growth in multiple PSMA-positive prostate cancer xenograft pharmacology models. In addition, the highly controlled and stable conjugation of AS269 to a selected site minimally disrupts the antibody structure and homogeneity, thereby promoting native mAb-like biochemical and biophysical properties, enhanced PK, and ARX517 stability. The HA114 site of conjugation was determined in earlier studies (12) to be a preferred site for stability for ADCs utilizing cleavable and noncleavable drug-linkers, while the polyethylene glycol linker decreases hydrophobicity, which decreases ADC systemic clearance (18), and the resulting payload pAF-AS269 is not an MDR pump substrate (19). Because of these design elements, preclinical ARX517 exposures at efficacious versus toxicologic doses demonstrate a wide therapeutic index and high systemic stability.

Previous studies (20) established a wider therapeutic index for ADCs built with this HA114 SAA site-specific platform (DAR2) versus a conventional cysteine conjugate (DAR4) containing the same linker and drug module. The conventional maleimide-conjugated DAR4 ADC exhibited instability with retro-Michael–mediated loss of drug-linker in human serum and reattachment to albumin, whereas the site-specific DAR2 ADC remained intact after 28 days in serum. The DAR2 SAA site-specific conjugate showed comparable *in vivo* efficacy but significantly reduced severity and persistence of rat toxicologic effects compared with the DAR4 random cysteine conjugate, resulting in an improved therapeutic index.

Multiple PSMA-targeted ADCs (PSMA-ADC, MLN-2704, and MEDI3726) have previously undergone clinical investigation in mCRPC, but all have been discontinued because of significant toxicity and/or a narrow therapeutic index (8, 9, 11). Two of these ADCs, MLN-2704 and MEDI3726, incorporated humanized versions of the same J591 anti–PSMA mouse antibody used in ARX517 (8, 11). In keeping with a stochastic conjugation approach, labile conjugation chemistry, and a cleavable linker, MLN-2704 displayed a $t_{1/2}$ of 2 days in cynomolgus monkeys (21) and 2.7 days in patients with mCRPC, associated with rapid payload DM1 deconjugation in circulation (11), making it difficult to achieve sufficient tumor exposures at tolerable doses. In contrast, ARX517 displayed a $t_{1/2}$ of 13.5 days in cynomolgus monkeys, suggesting that it has more native mAb-like clearance and increased stability and that increased exposures in patients will be possible at lower doses compared with previous PSMA-targeted ADCs.

Similarly, MEDI3726 exhibited a clinical $t_{1/2}$ ranging from 0.3 to 1.8 days in the phase I dose-escalation trial (8). In this trial, a

comprehensive LC/MS-MS–based dataset showed significant LC and HC dissociation occurring in patient circulation within a week of MEDI3726 administration (22). As noted by Huang and colleagues, by the end of the 3-week dosing interval, the majority of the ADCs were present as dissociated HC payload species that cannot bind PSMA target, which may cause undesirable toxicity and narrow the therapeutic index. Therefore, conjugation approaches that affect antibody interchain bond stability can have a significant effect on payload delivery to target-expressing tumor cells.

For the random cysteine-conjugated PSMA-ADC, the clinical $t_{1/2}$ was less than 2 days at the MTD, and the serum concentrations of free payload MMAE remained above the *in vitro* IC_{50} for cytotoxicity for at least 1 week following dosing in clinical trials (10, 23), which may imply that significant DTLs were related to off-target toxicities. In contrast, because of its site-specific engineering, stable conjugation chemistry, and payload cell impermeability, ARX517 dosing in cynomolgus monkeys resulted in maximum serum payload (pAF-AS269) concentrations >100-fold below the *in vitro* IC_{50} for cytotoxicity, thereby minimizing the potential for off-target toxicity.

Furthermore, the stability of ARX517 can ensure that every ADC molecule is fully loaded and able to deliver two molecules of toxin to the cancer cell. Once released inside the cell, the payload pAF-AS269 is non–cell permeable and not a substrate of MDR pumps, leading to accumulation of sufficient payload to kill the cancer cells.

ARX517 is built on the same site-specific conjugation platform and contains the same AS269 drug-linker as the HER2-targeted ADC ARX788, which has a $t_{1/2}$ of 10.6 days at the 10 mg/kg dose in cynomolgus monkeys and a clinical $t_{1/2}$ of 4 to 4.5 days at a dose of 1.5 mg/kg (24), further supporting the stability of our site-specific DAR2 noncleavable linker platform. For both ARX788 and ARX517, off-target tolerability was assessed in single-dose rat studies, in which common gross pathology and histopathology findings included (i) increased liver, spleen, and adrenal gland weight, (ii) decreased testes size/weight and hypospermia in epididymis, and (iii) alveolar macrophage accumulation in the lungs (25). Common clinical pathology findings included increased AST/ALT/CRE and reduced RBC/HGB/HCT. In repeat-dose monkey studies, common clinical pathology findings between ARX788 (once every three weeks for 4 doses, Q3Wx4) and ARX517 at any dose included changes in liver and kidney parameters (increases in AST/ALT/ALP/CRE, decreased ALB) and increased monocytes and coagulation times (APTT), and common histopathologic target organs were the spleen, kidneys, liver, thymus, and lungs. Taken together, data from ARX788 and ARX517 rat and monkey studies reveal common target-independent toxicologic profiles at high doses for DAR2 ADCs built on the site-specific AS269 technology. Although there were no major differences in these nonhuman primate off-target toxicology finding magnitudes or durations between the two ADCs, it is theoretically possible that low-level expression of ADC targets in select organs could amplify the aforementioned target-independent toxicities. Importantly, for both ARX517 and ARX788, antitumor activity was seen in mouse tumor models at much lower exposures than toxicities emerged in rat or primate toxicology models, indicating a wide therapeutic index.

PSMA is highly selectively expressed in prostate tissue and is overexpressed in the majority of prostate-derived tumors (5). Although the recent approval of the targeted radioligand therapy PLUVICTO is encouraging for patients with prostate cancer, PLUVICTO responses are often not complete. Although resistance mechanisms are not thoroughly understood, PSMA expression has been confirmed in a patient that progressed following PLUVICTO treatment (26), suggesting that ARX517 could potentially have clinical benefit after targeted radioligand therapy.

Interestingly, enzalutamide treatment increases PSMA expression in tumors (27, 28), suggesting that the coordinated or combination treatment of enzalutamide (or similar AR pathway inhibitors) with PSMA-targeted agents such as ARX517 could provide enhanced benefit. Accordingly, we observed additive efficacy upon combination of enzalutamide and ARX517 in enzalutamide-sensitive mouse tumor models. Although the additive *in vivo* efficacy of ARX517 and enzalutamide is encouraging, future studies are needed to understand the mechanistic underpinnings of this combination effect (e.g., *in vivo* PSMA upregulation, altered payload sensitivity, or differential effects on tumor subpopulations). Importantly, here we demonstrated that ARX517 can inhibit enzalutamide-resistant tumor growth *in vivo*.

The strategy to engineer ARX517 for stability should minimize the DLT mediated by premature release of payloads, which was observed with previous PSMA-targeted ADCs. Although the approach of using membrane-permeable drugs for bystander effect could potentially improve efficacy in heterogeneous tumor settings, it can come at the expense of causing toxicity to healthy cells, thereby narrowing the therapeutic index and potentially limiting combination options.

Additionally, ADCs with auristatin payloads, such as belantamab mafodotin and brentuximab vedotin, have demonstrated the capability to elicit immunogenic cell death in preclinical studies (29) and increase intratumoral $CD8^+$ T cells in patients (30). The ARX517 payload falls within this class of auristatin payloads, so it is possible that ARX517 may also induce immunogenic cell death and engage the immune system. This is an area for future investigation and may provide a rationale for ADC combination therapy with immune modulators or immune checkpoint therapies. In particular, the high stability of ARX517 should minimize off-target toxicity as demonstrated in our ARX788 program, making ARX517 an ideal agent for combination therapy. These data support the clinical evaluation of ARX517, as a phase I study in the United States (APEX-01, NCT04662580) is currently ongoing. In summary, the precision-engineered ADC ARX517 has demonstrated favorable stability in preclinical studies and a clear therapeutic index based on exposures at pharmacologically active doses versus the HNSTD in monkeys.

Authors' Disclosures

All authors were employees of Ambrx at the time the work was conducted. L.K. Skidmore reports a patent for US11420999 issued to Ambrx, Inc. N.A. Knudsen reports a patent for 20220033518 A1 pending. F. Tian reports a patent for US10800856 issued. No disclosures were reported by the other authors.

Authors' Contributions

L.K. Skidmore: Conceptualization, formal analysis, supervision, visualization, methodology, writing–original draft, project administration, writing–review and editing. **D. Mills:** Conceptualization, formal analysis, visualization, writing–original draft, writing–review and editing. **J.Y. Kim:** Conceptualization, formal analysis, investigation, visualization, methodology, writing–original draft, writing–review and editing. **N.A. Knudsen:** Formal analysis, supervision, investigation, visualization, methodology, writing–original draft, project administration, writing–review and editing. **J.D. Nelson:** Formal analysis, investigation, visualization, methodology, writing–original draft, writing–review and editing. **M. Pal:** Formal analysis, supervision, investigation, visualization, methodology, writing–

original draft, project administration, writing–review and editing. **J. Wang:** Conceptualization, supervision, visualization, methodology, writing–original draft, writing–review and editing. **K. GC:** Investigation, methodology, writing–original draft, writing–review and editing. **M.J. Gray:** Conceptualization, formal analysis, supervision, investigation, visualization, methodology, writing–original draft, project administration, writing–review and editing. **W. Barkho:** Formal analysis, investigation, visualization, methodology, writing–original draft, writing–review and editing. **P. Nagaraja Shastri:** Conceptualization, formal analysis, supervision, visualization, writing–original draft, project administration, writing–review and editing. **M.P. Ramprasad:** Conceptualization, supervision, methodology, project administration, writing–review and editing. **F. Tian:** Conceptualization, supervision, writing–review and editing. **D. O'Connor**: Conceptualization, writing–review and editing. **Y.J. Buechler:** Conceptualization, supervision, project administration, writing–review and editing. **S.S.-H. Zhang:** Conceptualization, supervision, project administration, writing–review and editing.

Note

Supplementary data for this article are available at Molecular Cancer Therapeutics Online (http://mct.aacrjournals.org/).

Received January 1, 2024; revised April 19, 2024; accepted August 15, 2024; published first August 22, 2024.

References

1. Siegel RL, Miller KD, Wagle NS, Jemal A. Cancer statistics, 2023. CA Cancer J Clin 2023;73:17–48.
2. Khoshkar Y, Westerberg M, Adolfsson J, Bill-Axelson A, Olsson H, Eklund M, et al. Mortality in men with castration-resistant prostate cancer—a long-term follow-up of a population-based real-world cohort. BJUI Compass 2022;3:173–83.
3. Lowrance W, Dreicer R, Jarrard DF, Scarpato KR, Kim SK, Kirkby E, et al. Updates to advanced prostate cancer: AUA/SUO guideline (2023). J Urol 2023;209:1082–90.
4. Queisser A, Hagedorn SA, Braun M, Vogel W, Duensing S, Perner S. Comparison of different prostatic markers in lymph node and distant metastases of prostate cancer. Mod Pathol 2015;28:138–45.
5. Hupe MC, Philippi C, Roth D, Kümpers C, Ribbat-Idel J, Becker F, et al. Expression of prostate-specific membrane antigen (PSMA) on biopsies is an independent risk stratifier of prostate cancer patients at time of initial diagnosis. Front Oncol 2018;8:623.
6. Sartor O, De Bono J, Chi KN, Fizazi K, Herrmann K, Rahbar K, et al. Lutetium-177–PSMA-617 for metastatic castration-resistant prostate cancer. N Engl J Med 2021;385:1091–103.
7. Liu H, Rajasekaran AK, Moy P, Xia Y, Kim S, Navarro V, et al. Constitutive and antibody-induced internalization of prostate-specific membrane antigen. Cancer Res 1998;58:4055–60.
8. de Bono JS, Fleming MT, Wang JS, Cathomas R, Miralles MS, Bothos J, et al. Phase I study of MEDI3726: a prostate-specific membrane antigen-targeted antibody-drug conjugate, in patients with mCRPC after failure of abiraterone or enzalutamide. Clin Cancer Res 2021;27:3602–9.
9. Petrylak DP, Vogelzang NJ, Chatta K, Fleming MT, Smith DC, Appleman LJ, et al. PSMA ADC monotherapy in patients with progressive metastatic castration-resistant prostate cancer following abiraterone and/or enzalutamide: efficacy and safety in open-label single-arm phase 2 study. Prostate 2020;80:99–108.
10. Petrylak DP, Kantoff P, Vogelzang NJ, Mega A, Fleming MT, Stephenson JJ, et al. Phase 1 study of PSMA ADC, an antibody-drug conjugate targeting prostate-specific membrane antigen, in chemotherapy-refractory prostate cancer. Prostate 2019;79:604–13.
11. Milowsky MI, Galsky MD, Morris MJ, Crona DJ, George DJ, Dreicer R, et al. Phase 1/2 multiple ascending dose trial of the prostate-specific membrane antigen (PSMA)-targeted antibody drug conjugate MLN2704 in metastatic castration-resistant prostate cancer. Urol Oncol 2016;34:530.e15–e21.
12. Tian F, Lu Y, Manibusan A, Sellers A, Tran H, Sun Y, et al. A general approach to site-specific antibody drug conjugates. Proc Natl Acad Sci U S A 2014;111:1766–71.
13. Tarantino P, Ricciuti B, Pradhan SM, Tolaney SM. Optimizing the safety of antibody–drug conjugates for patients with solid tumours. Nat Rev Clin Oncol 2023;20:558–76.
14. Bhomik S, Wang J, Xia J, Brady W, Tian F. Humanized anti-prostate-specific membrane antigen (PSMA) antibody drug conjugates. WO2019191728A1. 2019 Mar 29.
15. Smith-Jones PM, Vallabahajosula S, Goldsmith SJ, Navarro V, Hunter CJ, Bastidas D, et al. In vitro characterization of radiolabeled monoclonal antibodies specific for the extracellular domain of prostate-specific membrane antigen. Cancer Res 2000;60:5237–43.
16. Liu H, Moy P, Kim S, Xia Y, Rajasekaran A, Navarro V, et al. Monoclonal antibodies to the extracellular domain of prostate-specific membrane antigen also react with tumor vascular endothelium. Cancer Res 1997;57:3629–34.
17. Skidmore L, Sakamuri S, Knudsen NA, Hewet AG, Milutinovic S, Barkho W, et al. ARX788, a site-specific anti-HER2 antibody–drug conjugate, demonstrates potent and selective activity in HER2-low and T-DM1–resistant breast and gastric cancers. Mol Cancer Ther 2020;19:1833–43.
18. Lyon RP, Bovee TD, Doronina SO, Burke PJ, Hunter JH, Neff-LaFord HD, et al. Reducing hydrophobicity of homogeneous antibody-drug conjugates improves pharmacokinetics and therapeutic index. Nat Biotechnol 2015;33:733–5.
19. Barok M, Le Joncour V, Martins A, Isola J, Salmikangas M, Laakkonen P, et al. ARX788, a novel anti-HER2 antibody-drug conjugate, shows anti-tumor effects in preclinical models of trastuzumab emtansine-resistant HER2-positive breast cancer and gastric cancer. Cancer Lett 2020;473:156–63.
20. Jackson D, Atkinson J, Guevara CI, Zhang C, Kery V, Moon S-J, et al. In vitro and in vivo evaluation of cysteine and site specific conjugated herceptin antibody-drug conjugates. PLoS One 2014;9:e83865.
21. Bander NH, Carr FJ, Hamilton A, inventor; Cornell Research Foundation, Inc., assignee. Methods of treating prostate cancer with anti-prostate specific membrane antigen antibodies. US7514078B2. 2009 Apr 7.
22. Huang Y, Del Nagro CJ, Balic K, Mylott WR, Ismaiel OA, Ma E, et al. Multifaceted bioanalytical methods for the comprehensive pharmacokinetic and catabolic assessment of MEDI3726, an anti-prostate-specific membrane antigen pyrrolobenzodiazepine antibody-drug conjugate. Anal Chem 2020;92:11135–44.
23. Wang X, Ma D, Olson WC, Heston WDW. In vitro and in vivo responses of advanced prostate tumors to PSMA ADC, an auristatin-conjugated antibody to prostate-specific membrane antigen. Mol Cancer Ther 2011;10:1728–39.
24. Zhang J, Ji D, Shen W, Xiao Q, Gu Y, O'Shaughnessy J, et al. Phase I trial of a novel anti-HER2 antibody–drug conjugate, ARX788, for the treatment of HER2-positive metastatic breast cancer. Clin Cancer Res 2022;28:4212–21.
25. Nagaraja Shastri P, Zhu J, Skidmore L, Liang X, Ji Y, Gu Y, et al. Nonclinical development of next-generation site-specific HER2-targeting antibody-drug conjugate (ARX788) for breast cancer treatment. Mol Cancer Ther 2020;19:1822–32.
26. Khreish F, Wiessner M, Rosar F, Ghazal Z, Sabet A, Maus S, et al. Response assessment and prediction of progression-free survival by ^{68}Ga-PSMA-11 PET/CT based on tumor-to-liver ratio (TLR) in patients with mCRPC undergoing ^{177}Lu-PSMA-617 radioligand therapy. Biomolecules 2021;11:1099.
27. Staniszewska M, Fragoso Costa P, Eiber M, Klose JM, Wosniack J, Reis H, et al. Enzalutamide enhances PSMA expression of PSMA-low prostate cancer. Int J Mol Sci 2021;22:7431.
28. Rosar F, Dewes S, Ries M, Schaefer A, Khreish F, Maus S, et al. New insights in the paradigm of upregulation of tumoral PSMA expression by androgen receptor blockade: enzalutamide induces PSMA upregulation in castration-resistant prostate cancer even in patients having previously progressed on enzalutamide. Eur J Nucl Med Mol Imaging 2020;47:687–94.
29. Montes de Oca R, Alavi AS, Vitali N, Bhattacharya S, Blackwell C, Patel K, et al. Belantamab mafodotin (GSK2857916) drives immunogenic cell death and immune-mediated antitumor responses in vivo. Mol Cancer Ther 2021;20:1941–55.
30. Müller P, Martin K, Theurich S, Schreiner J, Savic S, Terszowski G, et al. Microtubule-depolymerizing agents used in antibody–drug conjugates induce antitumor immunity by stimulation of dendritic cells. Cancer Immunol Res 2014;2:741–55.